

Interactions of the $\chi_{c1}(4274)$ state with light mesons

A. L. M. Britto^{*}

*Centro de Ciências Exatas e Tecnológicas, Universidade Federal do Recôncavo da Bahia,
R. Rui Barbosa, Cruz das Almas, 44380-000, Bahia, Brazil
and Instituto de Física, Universidade Federal da Bahia,
Campus Universitário de Ondina, 40170-115, Bahia, Brazil*

L. M. Abreu[†]

*Instituto de Física, Universidade Federal da Bahia, Campus Universitário de Ondina, 40170-115, Bahia, Brazil
and Instituto de Física, Universidade de São Paulo,
Rua do Matão, 1371, CEP 05508-090, São Paulo, São Paulo, Brazil*

F. S. Navarra[‡]

Instituto de Física, Universidade de São Paulo, Rua do Matão, 1371, CEP 05508-090, São Paulo, São Paulo, Brazil



(Received 20 June 2023; accepted 6 November 2023; published 27 November 2023)

We investigate the interactions of the $\chi_{c1}(4274)$ state with light mesons in the hot hadron gas formed in heavy-ion collisions. The vacuum and thermally averaged cross sections of production of $\chi_{c1}(4274)$ accompanied by light pseudoscalar and light vector mesons as well as the corresponding inverse processes are estimated within the context of an effective Lagrangian approach. The results suggest non-negligible thermal cross sections, with larger magnitudes for most of the suppression reactions than those for production. This might be a relevant feature to be considered in the analysis of future data collected in heavy-ion collisions.

DOI: [10.1103/PhysRevD.108.096028](https://doi.org/10.1103/PhysRevD.108.096028)

I. INTRODUCTION

A few years ago, the LHCb Collaboration reported the observation of a charmoniumlike state named $\chi_{c1}(4274)$ in the amplitude analysis of the decay $B^+ \rightarrow J/\psi \phi K^+$. Its quantum numbers have been established to be $I^G(J^{PC}) = 0^+(1^{++})$ with statistical significance of 6.0σ , and its measured mass and width [1,2]

$$\begin{aligned} m &= 4273.3 \pm 8.3_{-3.6}^{+17.2} \text{ MeV}, \\ \Gamma &= 56 \pm 11_{-11}^{+8.0} \text{ MeV}, \end{aligned} \quad (1)$$

at 5.8σ significance. These values of mass and width are consistent with a previous measurement claimed by the CDF Collaboration [3]. In the words of the PDG [4], which

expresses the consensus in the field: “this state shows properties different from a conventional $q\bar{q}$ state and is a candidate for an exotic structure.” In this work, we will follow some recent papers in which the $\chi_{c1}(4274)$ has been treated as a meson molecule. However, it is still possible to interpret it as a conventional $c\bar{c}$ state (for a discussion, see [5]).

A great deal of effort has been made by the community in order to describe the properties and intrinsic quark configuration of the $\chi_{c1}(4274)$. We will briefly highlight some of the proposals. In Refs. [6,7], it was considered as a s -wave $c\bar{s}\bar{c}$ tetraquark state within the framework of QCD sum rules, and in [8,9] using the compact tetraquark model. Interestingly, in Ref. [10], the authors showed that the relativized quark model proposed by Godfrey and Isgur cannot account for the compact tetraquark configuration but for the conventional $\chi_{c1}(3^3P_1)$ state. On the other hand, the excited charmonium state configuration cannot be accommodated in the context of the 3P_0 model, as suggested in Ref. [11].

The color triplet and sextet diquark-antidiquark configuration was also employed by [12]. Contrasting with experimental results, Ref. [13] proposed that the $\chi_{c1}(4274)$ would correspond rather to two, almost degenerate, unresolved lines with $J^{PC} = 0^{++}, 2^{++}$.

^{*}andrebritto@ufrb.edu.br

[†]luciano.abreu@ufba.br

[‡]navarra@if.usp.br

Published by the American Physical Society under the terms of the Creative Commons Attribution 4.0 International license. Further distribution of this work must maintain attribution to the author(s) and the published article's title, journal citation, and DOI. Funded by SCOAP³.

From another interesting perspective, an analysis of the $\chi_{c1}(4274)$ as a p -wave bound state of $D_s D_{s0}(2317)$ was performed in a quasipotential Bethe-Salpeter equation approach, with a partial wave decomposition on spin parity [14]. This comes from the fact that the $\chi_{c1}(4274)$ mass is just 12 MeV below the $D_s \bar{D}_{s0}(2317)$ threshold. And since the quantum numbers of D_s and \bar{D}_{s0} [henceforth we denote $\bar{D}_{s0}(2317)$ simply by \bar{D}_{s0}] are 0^- and 0^+ , the binding mechanism between these two mesons must be in p wave and strong to form a bound state. However, via an effective approach, Ref. [15] argued that the partial decay widths of the $\chi_{c1}(4274)$ do not favor the p -wave bound state interpretation but indicates the possibility of a new state so-called $Y'(4274)$, which might be found in experiments such as Belle and Belle II. In the end, the intrinsic nature and the properties of the $\chi_{c1}(4274)$ are still a matter of debate, and more experimental and theoretical studies are really needed.

We believe that heavy-ion collisions provide a promising scenario to investigate the properties of exotic states [16]. As discussed in precedent works, at the end of the quark-gluon plasma phase, quarks coalesce to form all types of hadronic states. The exotic states are then formed and can interact with other light hadrons during the hadron gas phase [17–25]. Their final multiplicities will depend on the interaction cross sections, which, in turn, depend on the spatial configuration of the quarks. Meson molecules are larger and, therefore, have greater cross sections, which means that they will have a more prominent interaction with the hadronic medium than compact tetraquarks.

In this work, we investigate the interactions of the $\chi_{c1}(4274)$ state with light mesons within the context of an effective Lagrangian approach. The vacuum and thermally averaged cross sections of reactions involving the production of $\chi_{c1}(4274)$ accompanied by pseudoscalar mesons π , K , and η and vector mesons ρ , K^* , and ω as well as the corresponding inverse processes are estimated. We would like to emphasize the following.

- (i) The hadron gas formed in heavy-ion collisions lives for $\simeq 10$ fm, and the timescale of strong interactions is $\simeq 1$ fm. Therefore, the multiquark states (tetraquarks or molecules) will inevitably interact with the light hadrons of the medium.
- (ii) The careful study of the ratio $\chi_{c1}(3872)/\psi(2S)$ as a function of the system size published in [26] made even more clear that the final state interactions (i.e., interactions within the hadron gas) are crucial to understand the data [27] giving extra support to statement (i).
- (iii) Simplifying assumptions concerning these interactions such as the use of constant matrix elements or the use of geometrical arguments to estimate the cross sections are not sufficient. The collision energies are of the order of the temperature, i.e., $\simeq 100$ – 200 MeV. In this energy range, the cross

sections are still sensitive to resonance formation and other details of the interactions.

In view of these considerations, we will keep, as in previous works, trying to describe the multiquark interactions within the hadron gas with effective Lagrangians. In the next section, we will briefly describe the formalism employed in this work. In Sec. III, we calculate the interaction cross sections; in Sec. IV, we present the thermally averaged cross sections (called from now on simply thermal cross sections), which are the really relevant quantities for transport model calculations. Finally, in Sec. V, we present some conclusions.

II. FORMALISM

In this section, we will investigate the interactions of the $\chi_{c1}(4274)$ state with the lightest pseudoscalar mesons (π , K , and η) and with the lightest vector mesons (ρ , ω , and K^*). We will study the reactions $\chi_{c1}(4274) + (\pi, K, \eta, \rho, K^*, \omega) \rightarrow (\bar{D}_s D^{(*)}, D_{s0} D_s^{(*)}, D_{s0} D_{s0})$, as well as the inverse processes. The lowest-order Born diagrams that contribute to the processes of our interest are shown in Figs. 1 and 2. To calculate their respective amplitudes, we use an effective theory formalism in which the vector mesons are interpreted as dynamical gauge bosons of the hidden $U(N)_V$ local symmetry (see Refs. [18–21] for a more detailed discussion). In particular, the following effective Lagrangians involving the light and charmed mesons are employed:

$$\mathcal{L}_{PPV} = -ig_{PPV} \langle V^\mu [P, \partial_\mu P] \rangle, \quad (2)$$

$$\mathcal{L}_{VVP} = \frac{g_{VVP}}{\sqrt{2}} \varepsilon^{\mu\nu\alpha\beta} \langle \partial_\mu V_\nu \partial_\alpha V_\beta P \rangle, \quad (3)$$

where P and V are the matrices in $U(4)$ flavor space containing the pseudoscalar and vector meson fields in the physical basis:

$$P = \begin{pmatrix} \frac{\pi^0}{\sqrt{2}} + \frac{\eta'}{\sqrt{6}} + \frac{\eta}{\sqrt{3}} & \pi^+ & K^+ & \bar{D}^0 \\ \pi^- & -\frac{\pi^0}{\sqrt{2}} + \frac{\eta'}{\sqrt{6}} + \frac{\eta}{\sqrt{3}} & K^0 & D^- \\ K^- & \bar{K}^0 & \frac{2\eta'}{\sqrt{6}} - \frac{\eta}{\sqrt{3}} & D_s^- \\ D^0 & D^+ & D_s^+ & \eta_c \end{pmatrix}, \quad (4)$$

$$V = \begin{pmatrix} \frac{\rho^0}{\sqrt{2}} + \frac{\phi}{\sqrt{6}} + \frac{\omega}{\sqrt{3}} & \rho^+ & K^{*+} & \bar{D}^{*0} \\ \rho^- & -\frac{\rho^0}{\sqrt{2}} + \frac{\phi}{\sqrt{6}} + \frac{\omega}{\sqrt{3}} & K^{*0} & D^{*-} \\ K^{*-} & \bar{K}^{*0} & \frac{2\phi}{\sqrt{6}} - \frac{\omega}{\sqrt{3}} & D_s^{*-} \\ D^{*0} & D^{*+} & D_s^{*+} & J/\Psi \end{pmatrix}_\mu. \quad (5)$$

The construction of these physical states in terms of quarks is done using the parametrization discussed in Ref. [28] (see [29] for an interesting discussion on this subject) and also included in Appendix A. It is important to emphasize that the processes depicted in Figs. 1 and 2 include η , ρ , ω , and K^* but do not involve η' , η_c , ϕ , or J/ψ . These particles appear in the Lagrangians (2) and (3), but they have large masses. Since their abundances in the hadron gas are inversely proportional to their masses, they will be rare and will not contribute significantly to change the $\chi_{c1}(4274)$ multiplicity. For this reason, J/ψ and ϕ are not included in the calculations of $A + B \rightarrow C + D$ scatterings. However,

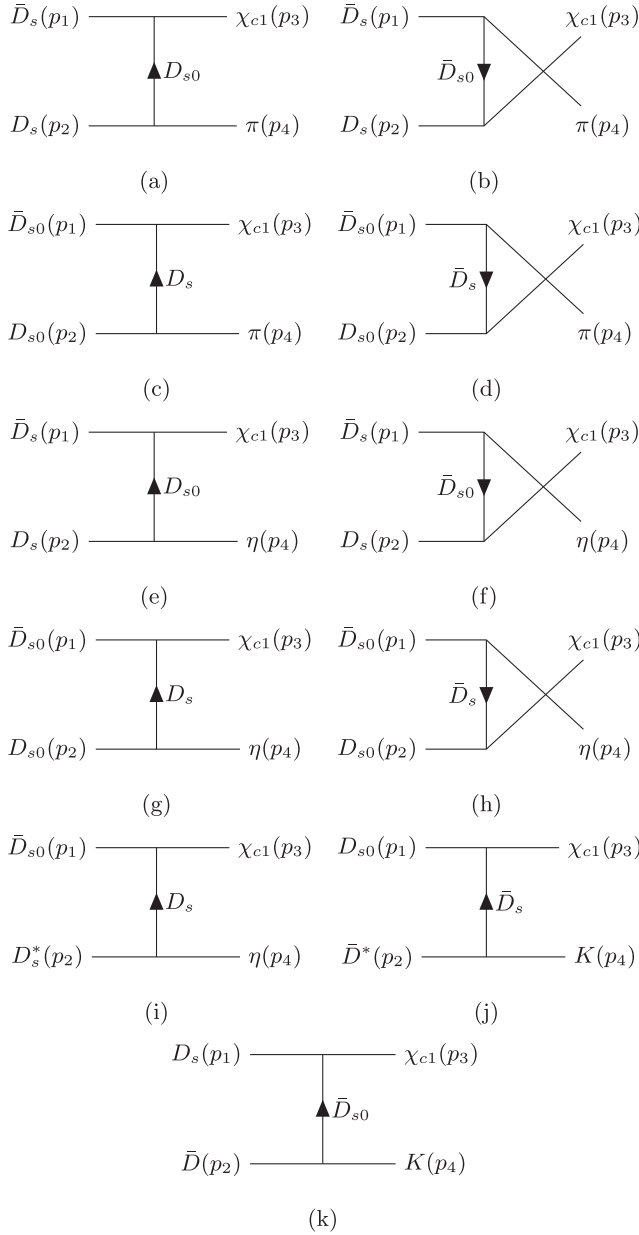


FIG. 1. Born diagrams describing the production of the $\chi_{c1}(4274)$ (denoted by χ_{c1}) and a light pseudoscalar meson (without specification of the charges of the particles).

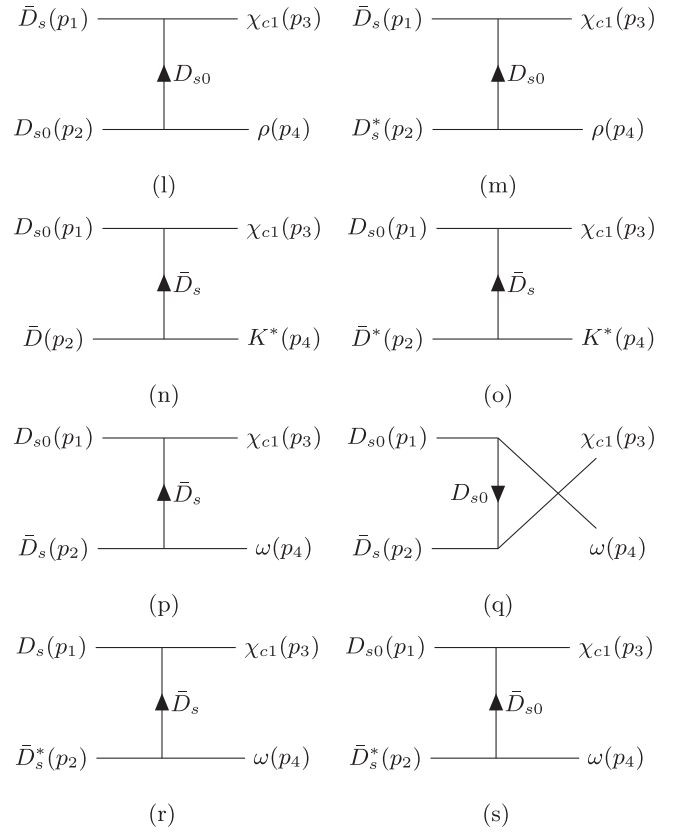


FIG. 2. Born diagrams describing the production of the $\chi_{c1}(4274)$ (denoted by χ_{c1}) and a light vector meson (without specification of the charges of the particles).

they must be included in the computation of the time evolution of the $\chi_{c1}(4274)$ multiplicity, because this state decays in the channel $Y \rightarrow J/\psi\phi$. This decay can be studied with a specific Lagrangian, and, since we have experimental data, we can extract the $YJ/\psi\phi$ coupling constant. So far, the only $\chi_{c1}(4274)$ decay channel that has been seen is $J/\psi\phi$. However, once one has a model of this state, it is possible to study theoretically other decay channels. In Ref. [15], using a molecular model of the $\chi_{c1}(4274)$, the authors calculated the decay width in the channels $J/\psi\phi$, $\chi_{c0}\eta$, $\chi_{c1}\eta$, $\bar{D}_s D_s^*$, $D\bar{D}^*$, $K\bar{K}^*$, and $\phi\phi$. These decays might be relevant to the calculation of the time evolution of the $\chi_{c1}(4274)$ multiplicity. This study is being performed and will appear in a forthcoming publication, where we use all the material presented here and, adding the information on the $Y \rightarrow J/\psi\phi$ decay, we solve the rate equation and calculate the time evolution of the $\chi_{c1}(4274)$ multiplicity.

The coupling constants are given by

$$g_{PPV} = \frac{m_V m_{D^*}}{2f_\pi m_{K^*}},$$

$$g_{VVP} = \frac{3m_V^2}{16\pi^2 f_\pi^3}, \quad (6)$$

with m_V being the mass of the vector meson; we take it as the mass of the ρ meson, and f_π is the pion decay constant. As pointed in Ref. [18], the factor m_{D^*}/m_{K^*} in the coupling g_{PPV} is introduced in order to reproduce the experimental decay width found for the process $D^* \rightarrow D\pi$ and comes from heavy-quark symmetry considerations.

Let us now introduce the vertex associated to the $\chi_{c1}(4274)$ state. The quantum numbers of $\chi_{c1}(4274)$ are $I(J^{PC}) = 0(1^{++})$, and those of D_s and D_{s0} are $J^P = 0^-$ and $J^P = 0^+$, respectively. Hence, for parity reasons, the vertex $\chi_{c1}D_sD_{s0}$ must be in relative P wave. This can be implemented by a term with a derivative coupling in the Lagrangian. The appropriate effective Lagrangian is then given by [15]

$$\mathcal{L}_{\chi_{c1}} = \frac{1}{\sqrt{2}} g_{\chi_{c1}D_s\bar{D}_{s0}} \chi_{c1}^\mu \left[D_s^+ \overleftrightarrow{\partial}_\mu D_{s0}^- - D_s^- \overleftrightarrow{\partial}_\mu D_{s0}^+ \right], \quad (7)$$

where χ_{c1}^μ stands for the field associated to the $\chi_{c1}(4274)$ state. The effective coupling constant $g_{\chi_{c1}D_s\bar{D}_{s0}}$ was taken from Ref. [15], in which the approach used was the compositeness condition. It is based on the idea that the renormalization constants of a composite particle wave function should be zero. By its turn, these renormalization constants carry on the self-energy of the $\chi_{c1}(4274)$ state, which naturally is written in terms of the coupling $g_{\chi_{c1}D_s\bar{D}_{s0}}$. Then, since the self-energy depends on a cutoff (q_{\max}), $g_{\chi_{c1}D_s\bar{D}_{s0}}$ was computed taking q_{\max} in the range 0.9–1.1 GeV. This resulted in $g_{\chi_{c1}D_s\bar{D}_{s0}} = 13.34_{-0.89}^{+1.11}$, where the central value corresponds to its value at $q_{\max} = 1.0$ GeV, and the errors to the variation of q_{\max} from 0.9 to 1.1 GeV.

Other couplings involving the D_{s0} state, charmed mesons, and light mesons present in the processes depicted in Figs. 1 and 2 are also needed. In the case of the light pseudoscalar mesons (in Fig. 1), the relevant three-body Lagrangians are [15] (we have used the same notation as in this reference)

$$\begin{aligned} \mathcal{L}_{KDD_{s0}} &= g_{KDD_{s0}} KDD_{s0}, \\ \mathcal{L}_{\pi^0 D_s D_{s0}} &= g_{\pi^0 D_s D_{s0}} \pi^0 D_s D_{s0}, \\ \mathcal{L}_{\eta D_s D_{s0}} &= g_{\eta D_s D_{s0}} \eta D_s D_{s0}, \end{aligned} \quad (8)$$

where the coupling constants are $g_{KDD_{s0}} = 10.21 \pm 1.13$ GeV, $g_{\eta D_s D_{s0}} = 6.40 \pm 1.15$ GeV, and $g_{\pi^0 D_s D_{s0}} = 1.3124_{-0.1385}^{+0.000}$ GeV. The central values of $g_{KDD_{s0}}$ and $g_{\eta D_s D_{s0}}$ were taken from the unitarized coupled-channel approach summarized in [30]; to take into account their uncertainties, we evaluated the difference between the values in the mentioned framework and their central values from a phenomenological model quoted in Table IX of [30]. $g_{\pi^0 D_s D_{s0}}$ was calculated using the upper limit of the D_{s0} width [15] and its uncertainty estimated from the upper

and lower limits of the absolute branching fraction of the decay $\Gamma(D_{s0}^\pm \rightarrow \pi^0 D_s^\pm)$ reported in [4].

For the three-body vertices involving the D_{s0} state, charmed mesons, and light vector mesons (in Fig. 2), we employ the following Lagrangians [31]:

$$\begin{aligned} \mathcal{L}_{VD_{s0}D_{s0}} &= -i g_{VD_{s0}D_{s0}} V^\mu D_{s0}^- \overleftrightarrow{\partial}_\mu D_{s0}^+, \\ \mathcal{L}_{VD_{s0}D_s^*} &= g_{VD_{s0}D_s^*} [D_{s0}^- D_{s\mu\nu}^{*+} - D_{s0}^+ D_{s\mu\nu}^{*-}] V^{\mu\nu}, \end{aligned} \quad (9)$$

where $V_{\mu\nu} = \partial_\mu V_\nu - \partial_\nu V_\mu$. The coupling constants $g_{VD_{s0}D_{s0}}$ and $g_{VD_{s0}D_s^*}$ are estimated through the vector dominance (VMD) model [31]. Accordingly, the virtual photon in the $D_{s0}^+ e^- \rightarrow D_{s0}^+ e^-$ scattering is coupled to the vector meson via the photon-vector-meson mixing term [31]

$$\mathcal{L}_{\gamma V} = \gamma_V V^\mu A_\mu, \quad (10)$$

where A_μ is the photon field; γ_V is the photon-vector-meson mixing amplitude. We remark that the form of the interaction in Eq. (10) does not preserve electromagnetic gauge invariance, and, because of this, the photon would acquire a mass unless we add a proper photon mass counterterm to the Lagrangian [32–34]. Besides, considering the example of the $\rho^0 - \gamma$ transition for the process $\gamma \rightarrow \pi^+ \pi^-$, the pion form factor $F_\pi(q^2)$ calculated with Eq. (10) will satisfy the condition of electromagnetic current conservation, $F_\pi(0) = 1$, only if the so-called universality condition is fulfilled, i.e., by demanding complete ρ dominance: $g_{\rho\pi\pi} = g_{\rho NN} = \dots = g_\rho$ [32–34]. Actually, the $U(1)_{\text{EM}}$ invariance is directly satisfied when we consider a different and more elegant version of the VMD Lagrangian, written as $\mathcal{L}_{\gamma V} \sim V^{\mu\nu} F_{\mu\nu}$ ($F_{\mu\nu}$ being the electromagnetic tensor); it is also in consonance with the current conservation condition without any assumption concerning the universality condition. For a more detailed discussion, we refer the reader to Refs. [32–34]. However, for our purposes, we proceed as usually done in the phenomenological approaches: The coupling in Eq. (10) is treated effectively, and γ_V is determined from the width of the vector-to-electron-positron decay:

$$\Gamma_V = \frac{\alpha_{em} \gamma_V^2}{3m_V^3}, \quad (11)$$

where α_{em} is the electromagnetic fine-structure constant and m_V is the vector mass. For the ω and ρ mesons we have $\Gamma_\omega = 0.60 \pm 0.02$ keV and $\Gamma_\rho = 7.04 \pm 0.06$ keV, respectively [4]. These values yield the following mixing amplitudes: $\gamma_\omega = 0.011$ GeV² and $\gamma_\rho = 0.037$ GeV².

Next, the coupling constants $g_{\omega D_{s0} D_{s0}}$ and $g_{\rho^0 D_{s0} D_{s0}}$ can be estimated with the following expression:

$$\frac{\gamma_V g_{VD_{s0}D_{s0}}}{m_V^2} = \frac{1}{3} e, \quad (12)$$

which gives $g_{\omega D_{s0}D_{s0}} = 5.50$ and $g_{\rho^0 D_{s0}D_{s0}} = 1.66$. To obtain $g_{VD_{s0}D_s^*}$, we make use of an extension of Eq. (12), i.e.,

$$\frac{\gamma_V g_{VD_{s0}D_s^*}}{m_V^2} = \frac{1}{3} e g_{\gamma D_{s0}D_s^*}, \quad (13)$$

where $g_{\gamma D_{s0}D_s^*}$ is the coupling constant of the vertex involving the photon, D_{s0} , and D_s^* , which from theoretical estimates is $g_{\gamma D_{s0}D_s^*} \geq 3.02 \times 10^{-2}$ GeV [31,35]. Therefore, we can write

$$g_{VD_{s0}D_s^*} = g_{VD_{s0}D_{s0}} \times g_{\gamma D_{s0}D_s^*}. \quad (14)$$

Taking the smallest value of $g_{\gamma D_{s0}D_s^*}$, we obtain $g_{\omega D_{s0}D_s^*} = 0.17$ GeV and $g_{\rho D_{s0}D_s^*} = 0.050$ GeV. Then, the effective model above allows us to write the amplitudes corresponding to the diagrams depicted in Figs. 1 and 2 as

$$\begin{aligned} M_{D_s D_s \rightarrow \chi_{c1} \pi} &= M^{(a)} + M^{(b)}, \\ M_{D_{s0} D_{s0} \rightarrow \chi_{c1} \pi} &= M^{(c)} + M^{(d)}, \\ M_{D_s D_s \rightarrow \chi_{c1} \eta} &= M^{(e)} + M^{(f)}, \\ M_{D_{s0} D_{s0} \rightarrow \chi_{c1} \eta} &= M^{(g)} + M^{(h)}, \\ M_{D_{s0} D_s^* \rightarrow \chi_{c1} \eta} &= M^{(i)}, \\ M_{D_{s0} D^* \rightarrow \chi_{c1} K} &= M^{(j)}, \\ M_{D_s D \rightarrow \chi_{c1} K^*} &= M^{(k)}, \\ M_{D_s D_{s0} \rightarrow \chi_{c1} \rho} &= M^{(l)}, \\ M_{D_s D_s^* \rightarrow \chi_{c1} \rho} &= M^{(m)}, \\ M_{D_{s0} D \rightarrow \chi_{c1} K^*} &= M^{(n)}, \\ M_{D_{s0} D^* \rightarrow \chi_{c1} K^*} &= M^{(o)}, \\ M_{D_{s0} D_s \rightarrow \chi_{c1} \omega} &= M^{(p)} + M^{(q)}, \\ M_{D_s D_s^* \rightarrow \chi_{c1} \omega} &= M^{(r)}, \\ M_{D_{s0} D_s^* \rightarrow \chi_{c1} \omega} &= M^{(s)}. \end{aligned} \quad (15)$$

The explicit expressions are described in Appendix B.

III. CROSS SECTIONS

We define the isospin-spin-averaged cross section in the center-of-mass (c.m.) frame for a given reaction $ab \rightarrow cd$ in Eq. (15) as

$$\sigma_{ab \rightarrow cd} = \frac{1}{64\pi^2 s} \frac{|\vec{p}_{cd}|}{|\vec{p}_{ab}|} \frac{1}{g_a g_b} \int d\Omega \sum_{S,I} |M_{ab \rightarrow cd}|^2, \quad (16)$$

where $g_{a,b} = (2I_{a,b} + 1)(2S_{a,b} + 1)$ is the degeneracy factor of the particles in the initial state; s is the squared center-of-mass energy; $|\vec{p}_{ab}|$ and $|\vec{p}_{cd}|$ are the moduli of the three-momenta in the c.m. frame of the initial and final particles, respectively. The summation is performed over the spin and isospin of the initial and final states, with the latter being rewritten in terms of the particle basis with the explicit charges of the particles in the initial state, i.e.,

$$\sum_I |M_{ab \rightarrow cd}|^2 \rightarrow \sum_{Q_a, Q_b} |M_{ab \rightarrow cd}^{(Q_1, Q_2)}|^2. \quad (17)$$

The cross sections of the corresponding inverse reactions are evaluated by means of the detailed balance relation:

$$g_a g_b |\vec{p}_{ab}|^2 \sigma_{ab \rightarrow cd} = g_c g_d |\vec{p}_{cd}|^2 \sigma_{cd \rightarrow ab}. \quad (18)$$

Furthermore, to take into account the finite size of the hadrons and to suppress the artificial growth of the cross sections at large momenta, we make use of a monopolelike form factor:

$$F(\vec{q}) = \frac{\Lambda^2}{\Lambda^2 + \vec{q}^2}, \quad (19)$$

where \vec{q} is the transferred three-momentum in $t(u)$ channel and Λ is the cutoff, which we choose to be $\Lambda = 2.0$ GeV. This type of form factor has been extensively employed in the literature, and a detailed discussion on its role is found in Ref. [23].

The calculations are done with the isospin-averaged masses reported in the PDG [4]. Besides, to take into account the uncertainties in the coupling constant $g_{\chi_{c1} D_s D_{s0}}$, the results are presented in terms of bands associated to the smallest and largest possible values of $g_{\chi_{c1} D_s D_{s0}}$.

The cross sections for the processes discussed in previous section are plotted in Figs. 3 and 4 as functions of the c.m. energy \sqrt{s} , as well as those for the corresponding inverse reactions. In the case of $\chi_{c1}(4274)$ production, all cross sections are endothermic, showing a fast growth in the region very close to the threshold, with the exception of the channel $D_{s0} D_{s0} \rightarrow \chi_{c1} \pi$. Considering the region up to 400 MeV above the corresponding thresholds, the different channels present a wide range of magnitudes $\sim 10^{-6} - 10^0$ mb. In particular, for the $\chi_{c1}(4274)$ production accompanied by pion and η mesons, the channel with initial state $D_s^0 \bar{D}_s^0$ yields the dominant contributions, while the other cases are at least one order of magnitude smaller. We also remark that the channels involving the kaon or K^* mesons give contributions of similar order. Besides, the reactions involving the ρ^0 mesons with the initial or final state $D_s \bar{D}_s^*$ present the smallest cross sections due to the smaller coupling constant of the $\rho D_{s0} D_s^*$ interaction.

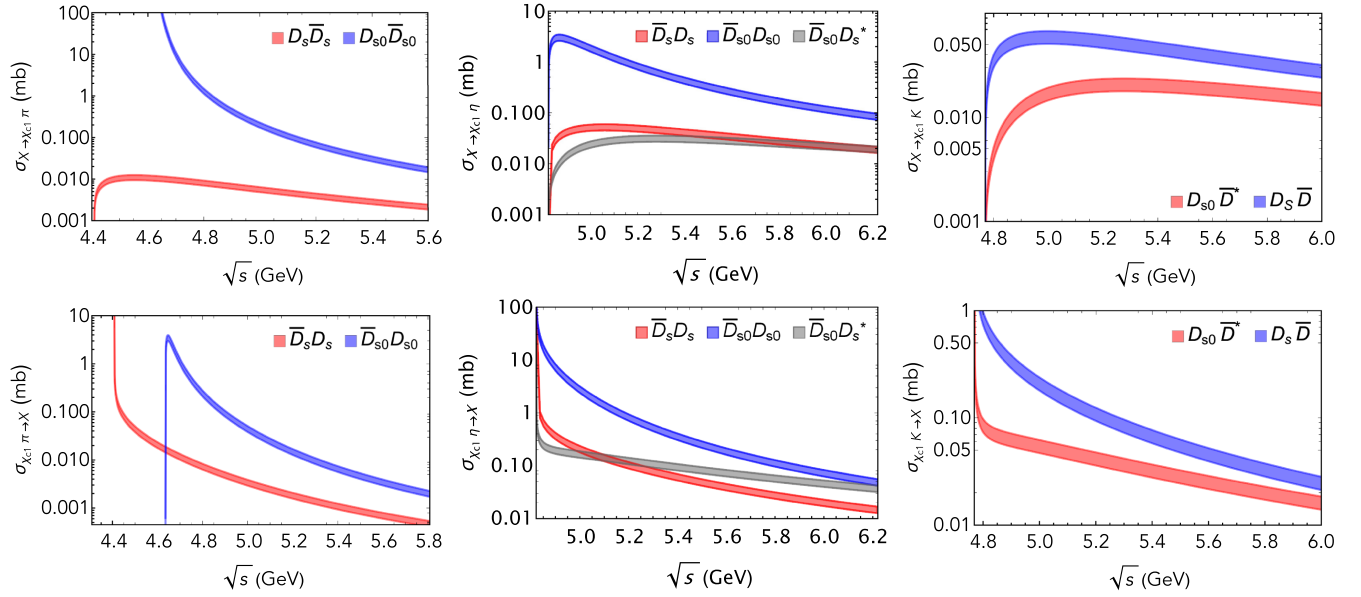


FIG. 3. Top: cross sections for the production processes $\chi_{c1}(4274)\pi$ (left), $\chi_{c1}(4274)\eta$ (center), and $\chi_{c1}(4274)K$ (right), as functions of \sqrt{s} . Bottom: cross sections for the corresponding inverse reactions.

Let us now look at the $\chi_{c1}(4274)$ -suppression processes in Figs. 3 and 4. As expected, only the process $\chi_{c1}\pi \rightarrow D_{s0}D_{s0}$ is endothermic; the other absorption cross sections are exothermic, becoming very large at the threshold. Above the threshold, these cross sections have very distinct magnitudes. Most importantly, when we compare $\chi_{c1}(4274)$ absorption and production by comoving light mesons in the relevant region of energies for heavy-ion collisions ($\sqrt{s} - \sqrt{s_0} < 0.6$ GeV), in general, the absorption cross sections are greater than the production ones. This feature

reflects the differences of these reactions concerning the phase space as well as the degeneracy factors encoded in Eq. (18).

IV. THERMAL CROSS SECTIONS

The findings of the previous sections allow us to go ahead and use them as input in the analysis of the $\chi_{c1}(4274)$ production and suppression in a heavy-ion collision environment, in which the medium effects become relevant.

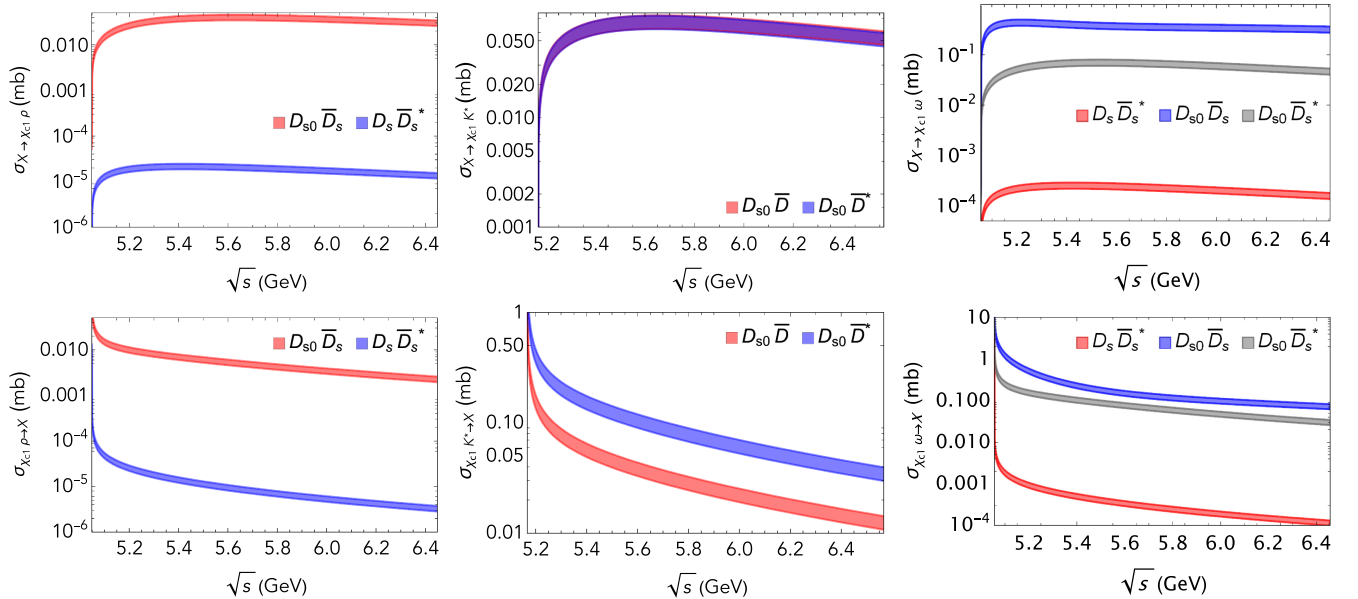


FIG. 4. Top: cross sections for the production processes $\chi_{c1}(4274)\rho$ (left), $\chi_{c1}(4274)K^*$ (center), and $\chi_{c1}(4274)\omega$ (right), as functions of \sqrt{s} . Bottom: cross sections for the corresponding inverse reactions. In the process $X \rightarrow \chi_{c1}K^*$, the curves are slightly overlapped.

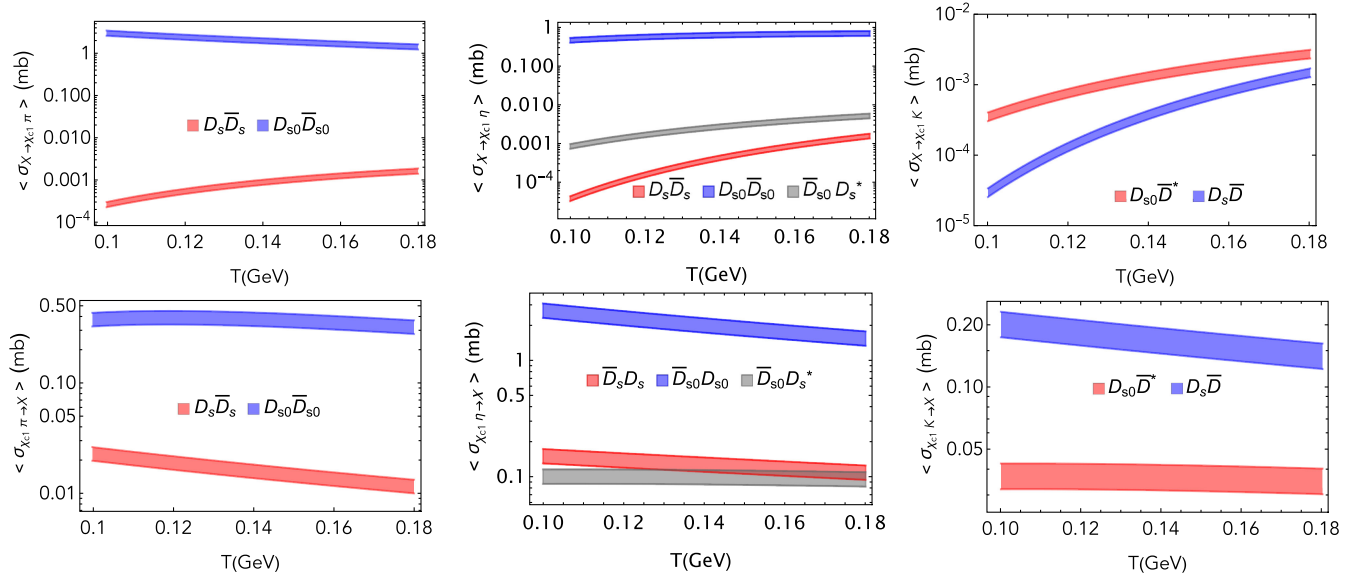


FIG. 5. Top: thermal cross sections for the production processes $\chi_{c1}(4274)\pi$ (left), $\chi_{c1}(4274)\eta$ (center), and $\chi_{c1}(4274)K$ (right), as functions of the temperature. Bottom: cross sections for the corresponding inverse reactions.

The collision energy is related to the temperature of the hadronic medium, and, hence, we need to evaluate the thermally averaged cross sections, which are defined as the cross sections averaged over the thermal distributions of the particles participating in the reactions. For the process $ab \rightarrow cd$, they are given by the convolution of vacuum cross sections and the momentum distributions:

$$\begin{aligned} \langle \sigma_{ab \rightarrow cd} v_{ab} \rangle &= \frac{\int d^3\mathbf{p}_a d^3\mathbf{p}_b f_a(\mathbf{p}_a) f_b(\mathbf{p}_b) \sigma_{ab \rightarrow cd} v_{ab}}{\int d^3\mathbf{p}_a d^3\mathbf{p}_b f_a(\mathbf{p}_a) f_b(\mathbf{p}_b)} \\ &= \frac{1}{4\beta_a^2 K_2(\beta_a) \beta_b^2 K_2(\beta_b)} \\ &\quad \times \int_{z_0}^{\infty} dz K_1(z) \sigma(s = z^2 T^2) \\ &\quad \times [z^2 - (\beta_a + \beta_b)^2][z^2 - (\beta_a - \beta_b)^2], \quad (20) \end{aligned}$$

where $f(p)$ is the Bose-Einstein distribution; v_{ab} is the relative velocity of the two initial particles a and b ; $\beta_i = m_i/T$, where T is the temperature; $z_0 = \max(\beta_a + \beta_b, \beta_c + \beta_d)$; and K_1 and K_2 are the modified Bessel functions of the second kind. In Figs. 5 and 6, we plot the thermal cross section as functions of the temperature. The suppression processes have a weaker dependence with the temperature than those for $\chi_{c1}(4274)$ production.

Comparing all the cross sections shown in the figures, the striking conclusion is that (unlike the case of most of the other exotic states) the most important process is $\chi_{c1}(4274)$ production through the reaction $D_{s0}\bar{D}_{s0} \rightarrow \chi_{c1}(4274)\pi$. The dominant absorption reaction is $\chi_{c1}(4274)\eta \rightarrow D_{s0}\bar{D}_{s0}$. In a hot hadron gas, the abundance of η is larger than the abundances of D_{s0} and \bar{D}_{s0} . This may compensate the difference in the cross sections, but at this point we

cannot say that there will be a $\chi_{c1}(4274)$ suppression due to hadronic medium effects. To know what really happens, we must solve the rate equations with the above cross sections. This will be addressed in a forthcoming publication.

V. CONCLUSIONS

In this work, we have studied the interactions of the $\chi_{c1}(4274)$ state with light mesons, which are the most abundant particles in the hot hadron gas formed in the late stage of heavy-ion collisions. Using an effective Lagrangian approach, we computed the vacuum and thermal cross sections of $\chi_{c1}(4274)$ production (accompanied by light pseudoscalar and vector mesons) and the corresponding inverse processes. The coupling constants involving the D_{s0} meson were calculated through the VMD model. The results show that the thermal cross sections are sizable. In almost all the cases, the absorption cross sections are larger than the production ones. However, the largest cross section is for $\chi_{c1}(4274)$ production through the reaction $D_{s0}\bar{D}_{s0} \rightarrow \chi_{c1}(4274)\pi$. Our study strongly motivates the use of the obtained cross sections as input to the rate equations, which yield the $\chi_{c1}(4274)$ multiplicity during the time evolution of a hot hadron gas. Work along this line is in progress.

ACKNOWLEDGMENTS

The authors thank Kanchan Khemchandani for the valuable discussions and providing her personal notes on the $U(4)$ formalism and $\eta - \eta' - \eta_c$ and $\omega - \phi - J/\psi$ mixings summarized in Appendix A. A. L. M. B. thanks H. P. L. Vieira for discussions. This work was partly supported by the Brazilian agencies Conselho Nacional

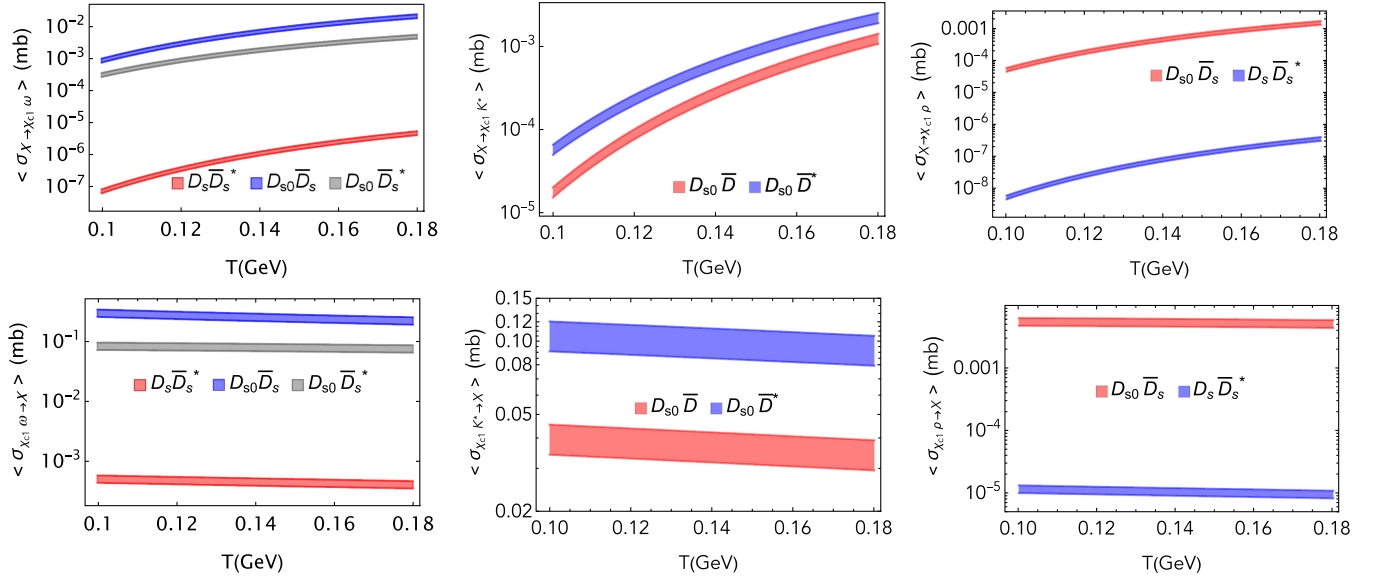


FIG. 6. Top: thermal cross sections for the production processes $\chi_{c1}(4274)\rho$ (left), $\chi_{c1}(4274)K^*$ (center), and $\chi_{c1}(4274)\omega$ (right), as functions of the temperature. Bottom: cross sections for the corresponding inverse reactions.

de Desenvolvimento Científico e Tecnológico (CNPq) under Contracts No. 309950/2020-1 (L. M. A.), No. 400215/2022-5 (L. M. A.), and 200567/2022-5 (L. M. A.) and CNPq/FAPERJ under the Project INCT-Física Nuclear e Aplicações (Contract No. 464898/2014-5).

APPENDIX A: THE $\eta - \eta' - \eta_c$ AND $\omega - \phi - J/\psi$ MIXING PATTERNS

Here, we discuss the parametrization for the matrices P and V given in Eq. (5), $\eta - \eta' - \eta_c$ and $\omega - \phi - J/\psi$ mixing patterns. Starting with the pseudoscalar mesons, the matrix P is defined in $U(4)$ flavor space by (see, for example, [30])

$$P = \begin{pmatrix} \frac{\pi^0}{\sqrt{2}} + \frac{\phi_0}{2} + \frac{\phi_8}{\sqrt{6}} + \frac{\phi_{15}}{\sqrt{12}} & \pi^+ & K^+ & \bar{D}^0 \\ \pi^- & -\frac{\pi^0}{\sqrt{2}} + \frac{\phi_0}{2} + \frac{\phi_8}{\sqrt{6}} + \frac{\phi_{15}}{\sqrt{12}} & K^0 & D^- \\ K^- & \bar{K}^0 & \frac{\phi_0}{2} - \frac{2\phi_8}{\sqrt{6}} + \frac{\phi_{15}}{\sqrt{12}} & D_s^- \\ D^0 & D^+ & D_s^+ & \frac{\phi_0}{2} - \frac{3\phi_{15}}{\sqrt{12}} \end{pmatrix}. \quad (\text{A2})$$

Then, choosing ϕ_0 , ϕ_8 , and ϕ_{15} as orthonormal states in the quark-antiquark basis according to the scenario in Ref. [30],

$$\begin{aligned} \phi_0 &= \frac{1}{2}(u\bar{u} + d\bar{d} + s\bar{s} + c\bar{c}), \\ \phi_8 &= \frac{1}{\sqrt{6}}(u\bar{u} + d\bar{d} - 2s\bar{s}), \\ \phi_{15} &= \frac{1}{\sqrt{12}}(u\bar{u} + d\bar{d} + s\bar{s} - 3c\bar{c}), \end{aligned} \quad (\text{A3})$$

$$P = \sum_{i=0}^{15} \frac{\phi_i}{\sqrt{2}} \lambda_i, \quad (\text{A1})$$

where $\lambda_a (a = 1, \dots, 15)$'s are the $SU(4)$ generators; $\lambda_0 = \text{diag}(1, 1, 1, 1)$; and the components ϕ_i are associated to the pseudoscalar states but are not necessarily the observed states. To construct the physical states, one can look into the quark content of each state. In the case of π , K , \bar{K} , D , and \bar{D} mesons, we use the standard relationship between the physical states and the quark content; therefore, Eq. (A1) reads

we get a null trace for the sum of fields associated to the $SU(4)$ generators, $\text{Tr}(\sum_{j=1}^{15} \frac{\phi_j}{\sqrt{2}} \lambda_j) = 0$, as expected.

In the scenario of Ref. [30], this mixing was not taken into account, and the physical states are just described by their most important components. However, experimental observations indicate the necessity of a mixing among the mathematical states ϕ_8 and ϕ_{15} belonging to $SU(4)$ and the singlet ϕ_0 in order to form the physical states η , η' , and η_c . See, for example, Refs. [36,37] for a discussion on the $\eta - \eta'$

mixing in $\eta/\eta' \rightarrow \gamma\gamma$ and other decays and Refs. [38,39] for the $\eta' - \eta_c$ mixing. In this sense, one can work in a more general framework and write the relationship between the physical states and mathematical states as

$$\begin{pmatrix} \eta \\ \eta' \\ \eta_c \end{pmatrix} = \begin{pmatrix} \cos\theta_P & -\sin\theta_P & 0 \\ \sin\theta_P & \cos\theta_P & 0 \\ 0 & 0 & 1 \end{pmatrix} \times \begin{pmatrix} 1 & 0 & 0 \\ 0 & \cos\theta_C & \sin\theta_C \\ 0 & \sin\theta_C & -\cos\theta_C \end{pmatrix} \begin{pmatrix} \phi_8 \\ \phi_0 \\ \phi_{15} \end{pmatrix}, \quad (\text{A4})$$

where θ_P and θ_C are the pseudoscalar mixing angles. Taking the considerations on the angle θ_P from Ref. [36], we fix $\theta_P = -20^\circ$, which gives $\cos\theta_P \approx 2\sqrt{2}/3$, $\sin\theta_P \approx -1/3$. Also, assuming that η and η' have a small contribution of the intrinsic charm content [38,39], we choose $\theta_C = 30^\circ$; then we have

$$\begin{aligned} \eta &= \frac{2\sqrt{2}}{3}\phi_8 + \frac{1}{2\sqrt{3}}\phi_0 + \frac{1}{6}\phi_{15}, \\ \eta' &= -\frac{1}{3}\phi_8 + \sqrt{\frac{2}{3}}\phi_0 + \frac{\sqrt{2}}{3}\phi_{15}, \\ \eta_c &= \frac{1}{2}\phi_0 - \frac{\sqrt{3}}{2}\phi_{15}. \end{aligned} \quad (\text{A5})$$

As a consequence, using Eq. (A3) in (A5), we obtain the physical states in terms of the quark-antiquark basis:

$$\begin{aligned} \eta &= \frac{1}{\sqrt{3}}(u\bar{u} + d\bar{d} - s\bar{s}), \\ \eta' &= \frac{1}{\sqrt{6}}(u\bar{u} + d\bar{d} + 2s\bar{s}), \\ \eta_c &= c\bar{c}. \end{aligned} \quad (\text{A6})$$

Hence, from Eq. (A5), the final form for the relations between the mathematical and physical bases reads

$$\begin{aligned} \frac{\phi_0}{2} + \frac{\phi_8}{\sqrt{6}} + \frac{\phi_{15}}{\sqrt{12}} &= \frac{\eta}{\sqrt{3}} + \frac{\eta'}{\sqrt{6}}, \\ \frac{\phi_0}{2} - \frac{2\phi_8}{\sqrt{6}} + \frac{\phi_{15}}{\sqrt{12}} &= -\frac{\eta}{\sqrt{3}} + \frac{2\eta'}{\sqrt{6}}, \\ \frac{1}{2}\phi_0 - \frac{3}{\sqrt{12}}\phi_{15} &= \eta_c, \end{aligned} \quad (\text{A7})$$

which allows one to rewrite the field P in Eq. (A1) in the physical basis as in Eq. (5).

The same considerations above can be made for the matrix of vector mesons, V_μ , given in Eq. (5). The pseudoscalar fields ϕ_i in Eq. (A1) should be replaced by

the vector fields ω_i , the physical pseudoscalar states in Eq. (A4) by the physical vector states ω , ϕ , and J/ψ and the mixing angle θ_P by θ_V . Assuming that ω acquires a small strange and charm content and that ϕ has a dominant strangeonium contribution [40], we fix $\theta_V \approx -55^\circ$ (giving $\cos\theta_V \approx 1/\sqrt{3}$, $\sin\theta_V \approx \sqrt{2/3}$), and obtain

$$\begin{aligned} \omega &= \frac{1}{\sqrt{3}}\omega_8 + \frac{1}{\sqrt{2}}\omega_0 + \frac{1}{\sqrt{6}}\omega_{15}, \\ \phi &= -\sqrt{\frac{2}{3}}\omega_8 + \frac{1}{2}\omega_0 + \frac{1}{\sqrt{12}}\omega_{15}, \\ J/\psi &= \frac{1}{2}\omega_0 - \frac{\sqrt{3}}{2}\omega_{15}. \end{aligned} \quad (\text{A8})$$

Thus, with the employment of similar relations as those in Eq. (A3) for the fields ω_a , the physical vector states in terms of the quark-antiquark basis read

$$\begin{aligned} \omega &= \frac{1}{\sqrt{2}}(u\bar{u} + d\bar{d}), \\ \phi &= s\bar{s}, \\ J/\psi &= c\bar{c}, \end{aligned} \quad (\text{A9})$$

and accordingly we obtain the final relationships which generate the matrix V in Eq. (5) in terms of the physical states:

$$\begin{aligned} \frac{\omega_0}{2} + \frac{\omega_8}{\sqrt{6}} + \frac{\omega_{15}}{\sqrt{12}} &= \frac{\omega}{\sqrt{3}} + \frac{\phi}{\sqrt{6}}, \\ \frac{\omega_0}{2} - \frac{2\omega_8}{\sqrt{6}} + \frac{\omega_{15}}{\sqrt{12}} &= -\frac{\omega}{\sqrt{3}} + \frac{2\phi}{\sqrt{6}}, \\ \frac{1}{2}\omega_0 - \frac{3}{\sqrt{12}}\omega_{15} &= J/\psi. \end{aligned} \quad (\text{A10})$$

APPENDIX B: AMPLITUDES

The explicit expressions of the amplitudes for the processes represented in Fig. 1 are

$$\begin{aligned} M^{(a)} &= -\frac{g_{\pi^0 D_s D_{s0}} g_{\chi_{c1} D_s \bar{D}_{s0}}}{\sqrt{2}} \epsilon^\mu(p_3) (p_3 - 2p_1)_\mu \frac{1}{t - m_{\bar{D}_{s0}}^2}, \\ M^{(b)} &= \frac{g_{\pi^0 D_s D_{s0}} g_{\chi_{c1} D_s \bar{D}_{s0}}}{\sqrt{2}} \epsilon^\mu(p_3) (p_3 - 2p_2)_\mu \frac{1}{u - m_{\bar{D}_{s0}}^2}, \\ M^{(c)} &= -\frac{g_{\pi^0 D_s D_{s0}} g_{\chi_{c1} D_s \bar{D}_{s0}}}{\sqrt{2}} \epsilon^\mu(p_3) (p_3 - 2p_1)_\mu \frac{1}{t - m_{\bar{D}_s}^2}, \\ M^{(d)} &= \frac{g_{\pi^0 D_s D_{s0}} g_{\chi_{c1} D_s \bar{D}_{s0}}}{\sqrt{2}} \epsilon^\mu(p_3) (p_3 - 2p_2)_\mu \frac{1}{u - m_{\bar{D}_s}^2}, \end{aligned}$$

$$\begin{aligned}
M^{(e)} &= -\frac{g_{\eta D_s D_{s0}} g_{\chi_{c1} D_s \bar{D}_{s0}}}{\sqrt{2}} \epsilon^\mu(p_3)(p_3 - 2p_1)_\mu \frac{1}{t - m_{D_{s0}}^2}, \\
M^{(f)} &= \frac{g_{\eta D_s D_{s0}} g_{\chi_{c1} D_s \bar{D}_{s0}}}{\sqrt{2}} \epsilon^\mu(p_3)(p_3 - 2p_2)_\mu \frac{1}{u - m_{D_{s0}}^2}, \\
M^{(g)} &= -\frac{g_{\eta D_s D_{s0}} g_{\chi_{c1} D_s \bar{D}_{s0}}}{\sqrt{2}} \epsilon^\mu(p_3)(p_3 - 2p_1)_\mu \frac{1}{t - m_{D_s}^2}, \\
M^{(h)} &= \frac{g_{\eta D_s D_{s0}} g_{\chi_{c1} D_s \bar{D}_{s0}}}{\sqrt{2}} \epsilon^\mu(p_3)(p_3 - 2p_2)_\mu \frac{1}{u - m_{D_s}^2}, \\
M^{(i)} &= \frac{g_{PPV} g_{\chi_{c1} D_s \bar{D}_{s0}}}{\sqrt{3}} \epsilon_\mu^*(p_2) \epsilon_\nu(p_3) \\
&\quad \times (p_2 - 2p_4)^\mu (p_3 - 2p_1)^\nu \frac{1}{t - m_{D_{s0}}^2}, \\
M^{(j)} &= \frac{g_{PPV} g_{\chi_{c1} D_s \bar{D}_{s0}}}{\sqrt{2}} \epsilon_\mu^*(p_2) \epsilon_\nu(p_3) \\
&\quad \times (-p_2 + 2p_4)^\mu (2p_1 - p_3)^\nu \frac{1}{t - m_{D_s}^2}, \\
M^{(k)} &= -\frac{g_{KDD_s} g_{\chi_{c1} D_s \bar{D}_{s0}}}{2} \epsilon^\mu(p_3)(-p_3 + 2p_1)_\mu \\
&\quad \times \frac{1}{t - m_{D_{s0}}^2}
\end{aligned}$$

and for those depicted in Fig. 2 are

$$\begin{aligned}
M^{(l)} &= -\frac{g_{\chi_{c1} D_s \bar{D}_{s0}} g_{\rho D_{s0} D_{s0}}}{\sqrt{2}} \epsilon(p_3)^\nu \epsilon(p_4)^\mu \\
&\quad \times (-2p_1 + p_4)_\mu (p_3 - 2p_2)_\nu \frac{1}{u - m_{D_{s0}}^2}, \\
M^{(m)} &= \frac{g_{\rho D_{s0} D_s} g_{\chi_{c1} D_s \bar{D}_{s0}}}{\sqrt{2}} (p_{4\mu} \epsilon_\nu^*(p_2) - p_{4\nu} \epsilon_\mu^*(p_2)) \\
&\quad \times (p_2^\nu \epsilon^\mu(p_4) - p_4^\mu \epsilon^\nu(p_4)) (2p_1 - p_3)_\rho \epsilon^\rho(p_3) \\
&\quad \times \frac{1}{t - m_{D_{s0}}^2},
\end{aligned}$$

$$\begin{aligned}
M^{(n)} &= \frac{g_{PPV} g_{\chi_{c1} D_s \bar{D}_{s0}}}{\sqrt{2}} \epsilon^\mu(p_4) \epsilon^\nu(p_3) \\
&\quad \times (p_4 - 2p_2)_\mu (2p_1 - p_3)_\nu \frac{1}{t - m_{D_s}^2}, \\
M^{(o)} &= \frac{g_{VVP} g_{\chi_{c1} D_s D_{s0}}}{2} \epsilon^{\mu\nu\alpha\beta} \epsilon^\rho(p_3) \epsilon^\beta(p_4) \epsilon^\nu(p_2) \\
&\quad \times (p_4)_\alpha (p_2)_\mu (2p_1 - p_3)_\rho \frac{1}{t - m_{D_s}^2}, \\
M^{(p)} &= -\frac{g_{PPV} g_{\chi_{c1} D_s \bar{D}_{s0}}}{\sqrt{3}} \epsilon(p_3)^\nu \epsilon(p_4)^\mu \\
&\quad \times (2p_2 - p_4)_\mu (2p_1 - p_3)_\nu \frac{1}{t - m_{D_s}^2}, \\
M^{(q)} &= \frac{g_{\chi_{c1} D_s \bar{D}_{s0}} g_{\omega D_{s0} D_s}}{\sqrt{2}} \epsilon(p_3)^\nu \epsilon(p_4)^\mu \\
&\quad \times (p_4 - 2p_1)_\mu (p_3 - 2p_2)_\nu \frac{1}{u - m_{D_{s0}}^2}, \\
M^{(r)} &= \frac{g_{\omega D_{s0} D_s} g_{\chi_{c1} D_s \bar{D}_{s0}}}{\sqrt{2}} (p_{4\mu} \epsilon_\nu^*(p_2) - p_{4\nu} \epsilon_\mu^*(p_2)) \\
&\quad \times (p_2^\nu \epsilon^\mu(p_4) - p_4^\mu \epsilon^\nu(p_4)) [(2p_1 - p_3)_\rho] \epsilon^\rho(p_3) \\
&\quad \times \frac{1}{t - m_{D_{s0}}^2}, \\
M^{(s)} &= \frac{g_{VVP} g_{\chi_{c1} D_s \bar{D}_{s0}}}{\sqrt{6}} \epsilon^{\mu\nu\alpha\beta} \epsilon^\rho(p_3) \epsilon^\nu(p_4) \epsilon^{\sigma\beta}(p_2) \\
&\quad \times (p_4)_\mu (p_2)_\alpha (-2p_1 + p_3)_\rho \frac{1}{t - m_{D_s}^2}.
\end{aligned}$$

In these expressions, p_1 and p_2 are the momenta of the initial states, and p_3 and p_4 are the momenta of the final states. The $\epsilon^\mu(p_i)$ is the polarization of vector states with momenta p_i ; u and t are the Mandelstam variables, which jointly with s are defined as follows: $s = (p_1 + p_2)^2$, $u = (p_1 - p_4)^2$, and $t = (p_1 - p_3)^2$.

-
- [1] R. Aaij *et al.* (LHCb Collaboration), *Phys. Rev. Lett.* **118**, 022003 (2017).
[2] R. Aaij *et al.* (LHCb Collaboration), *Phys. Rev. D* **95**, 012002 (2017).
[3] T. Aaltonen *et al.* (CDF Collaboration), *Mod. Phys. Lett. A* **32**, 1750139 (2017).
[4] R. L. Workman *et al.* (Particle Data Group), *Prog. Theor. Exp. Phys.* **2022**, 083C01 (2022).
[5] J. Ferretti, E. Santopinto, M. N. Anwar, and Y. Lu, *Eur. Phys. J. C* **80**, 464 (2020).
[6] H. X. Chen, E. L. Cui, W. Chen, X. Liu, and S. L. Zhu, *Eur. Phys. J. C* **77**, 160 (2017).
[7] Z. G. Wang, *Eur. Phys. J. C* **77**, 174 (2017).
[8] F. Stancu, *J. Phys. G* **37**, 075017 (2010); **46**, 019501(E) (2019).
[9] R. Zhu, *Phys. Rev. D* **94**, 054009 (2016).
[10] Q. F. Lü and Y. B. Dong, *Phys. Rev. D* **94**, 074007 (2016).
[11] L. C. Gui, L. S. Lu, Q. F. Lü, X. H. Zhong, and Q. Zhao, *Phys. Rev. D* **98**, 016010 (2018).
[12] S. S. Agaev, K. Azizi, and H. Sundu, *Phys. Rev. D* **95**, 114003 (2017).
[13] L. Maiani, A. D. Polosa, and V. Riquer, *Phys. Rev. D* **94**, 054026 (2016).
[14] J. He, *Phys. Rev. D* **95**, 074004 (2017).

- [15] H. Q. Zhu and Y. Huang, *Phys. Rev. D* **105**, 056011 (2022).
- [16] A. M. Sirunyan *et al.* (CMS Collaboration), *Phys. Rev. Lett.* **128**, 032001 (2022).
- [17] S. Cho and S. H. Lee, *Phys. Rev. C* **88**, 054901 (2013).
- [18] A. Martínez Torres, K. P. Khemchandani, F. S. Navarra, M. Nielsen, and L. M. Abreu, *Phys. Rev. D* **90**, 114023 (2014); *Acta Phys. Pol. B Proc. Suppl.* **8**, 247 (2015).
- [19] L. M. Abreu, K. P. Khemchandani, A. Martínez Torres, F. S. Navarra, and M. Nielsen, *Phys. Lett. B* **761**, 303 (2016).
- [20] L. M. Abreu, K. P. Khemchandani, A. Martínez Torres, F. S. Navarra, and M. Nielsen, *Phys. Rev. C* **97**, 044902 (2018).
- [21] L. M. Abreu, F. S. Navarra, and M. Nielsen, *Phys. Rev. C* **101**, 014906 (2020).
- [22] J. Hong, S. Cho, T. Song, and S. H. Lee, *Phys. Rev. C* **98**, 014913 (2018).
- [23] L. M. Abreu, F. S. Navarra, M. Nielsen, and H. P. L. Vieira, *Eur. Phys. J. C* **82**, 296 (2022).
- [24] L. M. Abreu, F. S. Navarra, and H. P. L. Vieira, *Phys. Rev. D* **105**, 116029 (2022).
- [25] L. M. Abreu, F. S. Navarra, and H. P. L. Vieira, *Phys. Rev. D* **106**, 076001 (2022).
- [26] A. M. Sirunyan *et al.* (CMS Collaboration), *Phys. Rev. Lett.* **128**, 032001 (2022); R. Aaij *et al.* (LHCb Collaboration), *Phys. Rev. Lett.* **126**, 092001 (2021).
- [27] Y. Guo, X. Guo, J. Liao, E. Wang, and H. Xing, [arXiv:2302.03828](https://arxiv.org/abs/2302.03828).
- [28] D. Gamermann, Meson resonances in the open and hidden charm sectors, Ph.D. thesis, http://ific.uv.es/nucth/tesis_DanGam.pdf.
- [29] W. I. Eshraim, F. Giacosa, and D. H. Rischke, *Eur. Phys. J. A* **51**, 112 (2015).
- [30] D. Gamermann, E. Oset, D. Strottman, and M. J. Vicente Vacas, *Phys. Rev. D* **76**, 074016 (2007).
- [31] Y.-L. Ma, *Phys. Rev. D* **82**, 015013 (2010).
- [32] J. J. Sakurai, *Currents and Mesons* (University of Chicago Press, Chicago, 1969).
- [33] H. B. O'Connell *et al.*, *Prog. Nucl. Part. Phys.* **39**, 201 (1997).
- [34] F. Jegerlehner and R. Szafron, *Eur. Phys. J. C* **71**, 1632 (2011).
- [35] A. Faessler, T. Gutsche, V. E. Lyubovitskij, and Y. L. Ma, *Phys. Rev. D* **76**, 014005 (2007).
- [36] F. J. Gilman and R. Kauffman, *Phys. Rev. D* **36**, 2761 (1987); **37**, 3348(E) (1988).
- [37] G. Amelino-Camelia, F. Archilli, D. Babusci, D. Badoni, G. Bencivenni, J. Bernabeu, R. A. Bertlmann, D. R. Boito, C. Bini, C. Bloise *et al.*, *Eur. Phys. J. C* **68**, 619 (2010).
- [38] B. Bagchi, P. Bhattacharyya, S. Sen, and J. Chakrabarti, *Phys. Rev. D* **60**, 074002 (1999).
- [39] M. Z. Yang and Y. D. Yang, *Nucl. Phys.* **B609**, 469 (2001).
- [40] A. Kucukarslan and U. G. Meissner, *Mod. Phys. Lett. A* **21**, 1423 (2006).